

## Original Article

# Modulation of mesenchymal stem cells with miR-375 to improve their therapeutic outcome during scar formation

Wei Sheng<sup>1\*</sup>, Zihao Feng<sup>2\*</sup>, Qi Song<sup>3</sup>, Heyong Niu<sup>4</sup>, Guoying Miao<sup>4</sup>

<sup>1</sup>Wound Care Center, College of Life Sciences, Chinese PLA General Hospital, Beijing 100853, China; <sup>2</sup>Department of Plastic and Reconstructive Surgery, Zhongshan Hospital, Fudan University, Shanghai 200032, China; <sup>3</sup>Department of Oncology, Chinese PLA General Hospital, Beijing 100853, China; <sup>4</sup>Department of Dermatology, Affiliated Hospital of Hebei University of Engineering, Handan 056029, China. \*Equal contributors.

Received February 9, 2016; Accepted March 6, 2016; Epub May 15, 2016; Published May 30, 2016

**Abstract:** Understanding of the mechanism of cutaneous scar formation with the goal of developing potential therapies to promote scar-less wound healing appears to be extremely critical. Mesenchymal stem cells (MSCs) have a demonstrate role in promoting scar-less wound healing. However, recent studies have shown that the function of MSCs may be attenuated due to insufficient activation in vivo. Here, we aimed to increase the activity and functions of MSCs to improve their effects during scar formation. We found that overexpression of microRNA-375 (miR-375) in MSCs significantly decreased the levels of tissue inhibitor of metalloproteinases 1 (TIMP-1) protein, but not mRNA. Mechanistically, miR-375 inhibited TIMP-1 protein translation through binding to the 3'-UTR of the TIMP-1 mRNA in MSCs. Transplantation of miR-375-expressing MSCs significantly reduced the fibrosis in the scar region of the mice, possibly through reduction of reactive oxygen species (ROS), suppression of transition of myofibroblasts from fibroblasts, and increases in hepatic growth factor (HGF). Together, these data suggest that overexpression of miR-375 in MSCs may substantially improve the effects of MSCs on reduction of scar during wound healing. Our study sheds new light on a scar-less wound healing.

**Keywords:** Scar formation, mesenchymal stem cells (MSCs), tissue inhibitor of metalloproteinases 1 (TIMP-1), miR375

## Introduction

Scars are a consequence of cutaneous wound healing generated by excessive deposition of extracellular matrix tissue by wound healing fibroblasts and myofibroblasts, with capability to restore integrity of the body boundary [1-3]. Besides having an undesirable visual appearance, the tissue in the vicinity of the scar does not function like the surrounding skin due to lack of necessary structures that are native to the dermis [1-3]. Moreover, the scar tissue is also limited to approximately 80% of the skin tensile strength, resulting in a susceptibility to re-injury [1-3]. Thus, understanding of the mechanism of cutaneous scar formation with the goal of developing potential therapies to promote scar-less wound healing appears to be extremely critical.

Mesenchymal stem cells (MSCs) have been initially identified in the bone marrow, and are the stem-like cells that expand in culture and may differentiate into osteoblasts, chondrocytes, and adipocytes [4-10]. Clinical data provide evidence to demonstrate a therapeutic effect of transplantation of MSCs in many inflammatory diseases through various mechanisms [5-10]. The versatility of MSCs has thus made them an attractive candidate for clinical translation in a variety of therapeutic applications. For example, MSCs may participate in normal wound healing through production and secretion of trophic mediators of tissue repair [11-15]. Moreover, MSCs may attenuate inflammation in the wound and reprogramming the resident immune and wound healing cells to favor tissue regeneration and inhibit fibrotic tissue formation [16]. In particular, MSCs may offer the

means of recapitulating several mechanisms that are sufficient for inhibition of scar formation in skin wounds [16]. As a result, MSCs have been considered and tested as a likely candidate for a cellular therapy to promote scar-less wound healing. However, recent studies have shown that the function of MSCs may be attenuated due to insufficient activation in vivo [17].

Tissue inhibitor of metalloproteinases 1 (TIMP-1) is a glycoprotein ubiquitously expressed in various human cells and tissues [18-20]. TIMP-1 controls the activity of MMPs and appears to an important regulator of extracellular matrix turnover [18-20]. Moreover, TIMP-1 also regulates cellular processes including cell growth, apoptosis, and differentiation that are independent of its metalloproteinase inhibitory activity [18-20]. Recently, TIMP-1 has been shown to be a negative regulator for MSC activity, and suppression of TIMP-1 may increase the potential therapeutic effects of MSCs during scar formation [17].

MicroRNAs (miRNAs) are non-coding small RNAs that regulate of the protein translation through their base-pairing with the 3'-untranslated region (3'-UTR) of the target mRNAs [21, 22]. It is well-known that miRNAs regulate different biological processes physiologically and pathologically [23-25]. Among all miRNAs, miR-375 has been relatively extensively studied, and has been shown to be involved in the pathogenesis of various diseases [26-29]. However, a role of miR-375 in modification of MSCs to facilitate its function in prevention of scar formation has not been acknowledged.

Here, we aimed to increase the activity and functions of MSCs to improve their effects during scar formation. We found that overexpression of miR-375 in MSCs significantly decreased the levels of TIMP-1 protein, but not mRNA. Mechanistically, miR-375 inhibited TIMP-1 protein translation through binding to the 3'-UTR of the TIMP-1 mRNA in MSCs. Transplantation of miR-375-expressing MSCs significantly reduced the fibrosis in the scar region of the mice, possibly through reduction of reactive oxygen species (ROS), suppression of transition of myofibroblasts from fibroblasts, and increases in hepatic growth factor (HGF). Together, these data suggest that overexpression of as-miR-375 in MSCs may substantially improve the therapeutic effects of MSCs on AD,

possibly through augmenting TIMP-1 levels in MSCs. Our study should have therapeutic implications for treating AD.

### Materials and methods

#### *Animals*

Female 12 week-old C57BL/6 mice were purchased from Jackson Laboratories (Bar Harbor, ME, USA). These mice were maintained at  $22 \pm 1^\circ\text{C}$ , under a 12-hour light/dark cycle, with free access to standard food and water. All experimental procedures were in strict accordance with the guidance for the Care and Use of Laboratory Animals, issued by Chinese PLA General Hospital, and proved by the research committee of Chinese PLA General Hospital. For induction of a scar, an injury of 2 cm long and 2 mm thick was made with a blade on the back of the mice.

#### *Preparation, differentiation and transduction of MSCs*

Bone-marrow derived MSCs from male 8-week-old C57BL/6 mice (Jackson Laboratories) were collected from femurs and tibias by flushing with culture medium (DMEM, Dulbecco's Modified Eagle's Medium, Gibco, San Diego, CA, USA). The cells were centrifuged and re-suspended in DMEM low glucose containing inactivated 10% fetal bovine serum (FBS), Gibco, 3.7 g/l HEPES (N-2-hydroxyethylpiperazine-N'-2-ethane-sulphonic acid, Sigma-Aldrich, St. Louis, MO, USA), 1% 200 mmol/l L-glutamine 100x (Gibco) and 1% PSA (Gibco). The cell number and viability were determined by trypan blue staining (Gibco) and reached a final cell density of  $5 \times 10^6$  cells/ml. The cells were incubated in a humidified chamber with 5% CO<sub>2</sub> at 37°C for 72 h, and the adherent cells, which were considered MSCs, were maintained in culture until reaching ~80% semi-confluence. Then, the MSCs were washed, incubated with trypsin-ethylenediamine-tetraacetic acid (EDTA) (StemCell Technologies, Vancouver, Canada) and prepared to be frozen with a cryoprotectant solution of dimethylsulphoxide (DMSO, MP Biomedicals, Santa Ana, USA) and FBS.

MSCs were transduced with an adeno-associated virus (AAV) carrying miR-375 and GFP construct (connected with an IRES sequence), or

## MSCs-miR-375 to prevent scar formation

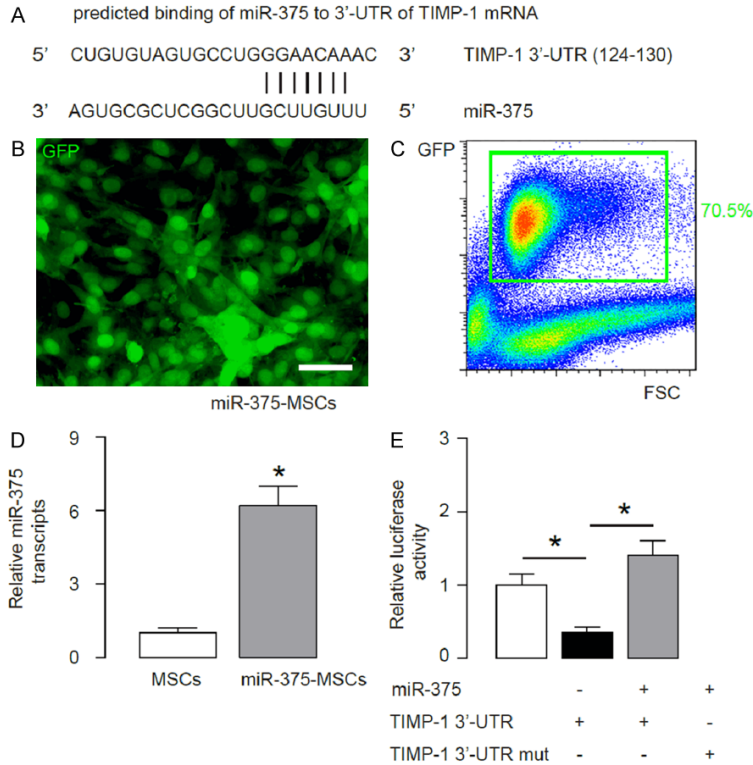


**Figure 1.** Preparation of miR-375-expressing MSCs. **A.** Bioinformatics showing that miR-375 binds to 3'-UTR of TIMP-1 mRNA at 124th-130th base site in MSCs. **B.** Transduced MSCs with miR-375 (miR-375-MSCs) by AAV in culture. The virus also carries a GFP reporter, and all the transduced cells expressed GFP. The control MSCs received AAV-null. **C.** The GFP-expressing transduced cells were purified by flow cytometry based on GFP, shown by representative flow chart. **D.** The levels of miR-375 in miR-375-MSCs by RT-qPCR. **E.** MSCs cells were then transfected with 1  $\mu$ g plasmids of miR-375-expressing plasmids and plasmids carrying a luciferase reporter for 3'-UTR of TIMP-1 mRNA or a luciferase reporter for 3'-UTR of TIMP-1 mRNA with mutate at the miR-375 binding site (mut). The luciferase activities were determined in these cells. \* $p < 0.05$ . N=5. Scale bar is 20  $\mu$ m.

control AAV (GFP sequence only; control). The sequence for as-miR-375 is 5'-gcgacgagccc-cucgcacaaac-3'. GFP allows purification of the transduced cells by flow cytometry based on green fluorescence. Human embryonic kidney 293 cell line (HEK293) was used for virus production. We used a pAAV-CMV-GFP plasmid (Clontech, Mountain View, CA, USA), a packaging plasmid carrying the serotype 8 rep and cap genes, and a helper plasmid carrying the adenovirus helper functions (Applied Viromics, LLC, Fremont, CA, USA) in this study. AAVs were prepared by triple transfection of the newly prepared plasmids, R2C8 (containing AAV2 Rep and AAV8 capsid genes) and pAd5 (containing adenovirus helper genes) into HEK293 cells by Lipofectamine 2000 reagent (Invitrogen, St. Louis, MO, USA). The viruses were purified

using CsCl density centrifugation and then titered by a quantitative densitometric dot-blot assay. Then, the MSCs cells were incubated with AAVs at a MOI of 100 for 12 hours to transduce the cells. Afterwards, transduced cells were purified by flow cytometry based on GFP expression.

A positive clone was selected after subjection to chondrogenetic, osteogenic, and adipogenic differentiation assays to confirm phenotype. For chondrogenetic induction,  $2.5 \times 10^5$  MSCs were induced with 5 ml chondrogenetic induction medium containing 10  $\mu$ g transforming growth factor  $\beta$ 1 (R&D System, Los Angeles, CA, USA), 50  $\mu$ g insulin growth factor 1 (R&D System, Los Angeles, CA, USA), and 2 mg/ml dexamethasone (DMSO, Sigma-Aldrich, St. Louis, MO, USA) followed by centrifugation at 500 g for 5 min. The cell pellets were maintained in the chondrogenetic induction medium for 14 days and subjected to Alcian blue staining. For osteogenic induction, cells were digested and seeded onto a 24-well plate at a

density of  $10^4$  cells/well, and then maintained in osteogenic induction medium containing 10 nM Vitamin D3 (Sigma-Aldrich) and 10 mM  $\beta$ -phosphoglycerol and 0.1  $\mu$ M DMSO for 14 days and were subjected to Von kossa staining. For adipogenic induction, cells were digested and seeded onto a 24-well plate at a density of  $10^4$  cells/well, and then maintained in the adipogenic induction medium containing 0.5 mmol/l 3-isobutyl-1-methylxanthine (IBMX), 200  $\mu$ mol/l indomethacin, 10  $\mu$ mol/l insulin and 1  $\mu$ mol/l DMSO for 14 days and subjected to Oil red O staining.

### Cell transplantation

Three days before the C57/BL6 mice at 12 weeks of age (n=10 per group) received injury

## MSCs-miR-375 to prevent scar formation

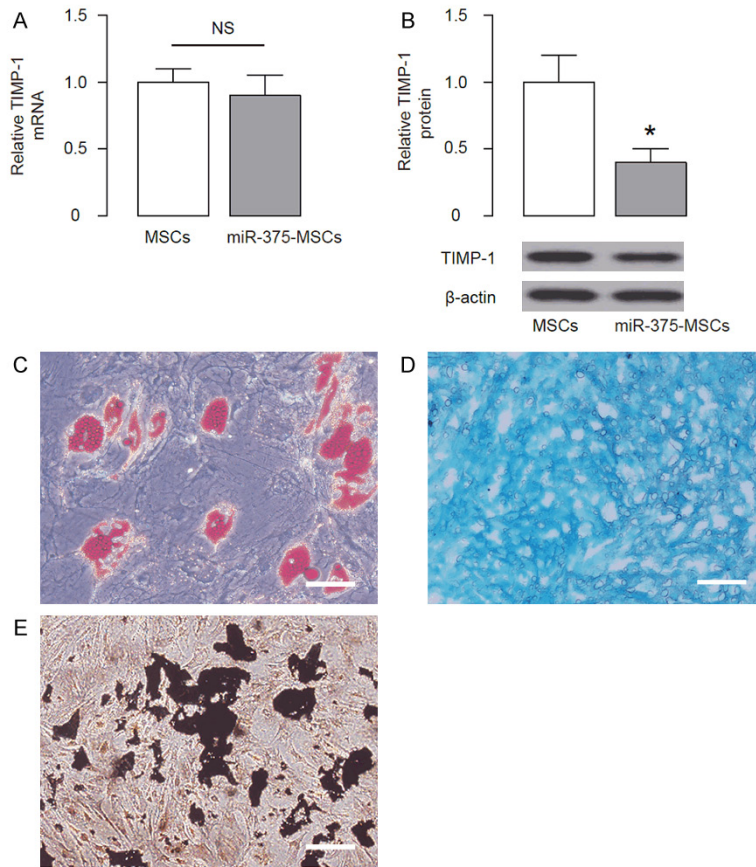


**Figure 2.** miR-375-MSCs express reduced levels of TIMP-1. (A, B) The TIMP-1 levels in miR-375-MSCs, by mRNA (A), and by Western blot (B). (C-E) Differentiation assays to confirm the MSC-phenotype after miR-375 overexpression. (C) Von kossa staining to evaluate osteogenic induction. (D) Oil red O staining to evaluate adipogenic induction. (E) Alcian blue staining to evaluate chondrogenetic induction. \* $p < 0.05$ . NS: non-significant.  $N=5$ . Scale bars are 100  $\mu\text{m}$ .

on the back, and  $10^6$  miR-375-MSCs or control MSCs in a 200  $\mu\text{l}$  PBS were injected into the tail vein of the mice. After injection, the mice were kept warm for 20 minutes, and then returned to their home cages.

### Histology

Masson-trichrome staining was performed using a Trichrome Stain (Masson) Kit (Sigma-Aldrich, St. Louis, MO, USA).

### Western blot

The protein was extracted from the tissue in the scar region and homogenized in RIPA lysis buffer (1% NP40, 0.1% SDS, 100  $\mu\text{g}/\text{ml}$  phenyl-methylsulfonyl fluoride, 0.5% sodium deoxycholate, in PBS) on ice. The supernatants were col-

lected after centrifugation at  $12000\times g$  at  $4^\circ\text{C}$  for 20 min. Protein concentration was determined using a BCA protein assay kit (Bio-rad, China), and whole lysates were mixed with 4 $\times$ SDS loading buffer (125 mmol/l Tris-HCl, 4% SDS, 20% glycerol, 100 mmol/l DTT, and 0.2% bromophenol blue) at a ratio of 1:3. Protein samples were heated at  $100^\circ\text{C}$  for 5 min and were separated on SDS-polyacrylamide gels. The separated proteins were then transferred to a PVDF membrane. The membrane blots were first probed with a primary antibody. After incubation with horseradish peroxidase-conjugated second antibody, autoradiograms were prepared using the enhanced chemiluminescent system to visualize the protein antigen. The signals were recorded using X-ray film. Primary antibodies for Western Blot are rat anti-TIMP-1, anti-ROS, anti-alpha smooth muscle actin ( $\alpha$ -SMA), anti-transforming growth factor beta (TGF $\beta$ ), anti-Collagen I, anti-Fibronectin and rabbit anti- $\beta$ -actin (Cell Signaling, San Jose, CA,

USA).  $\beta$ -actin was used as a protein loading control. The secondary antibody was HRP-conjugated anti-rabbit (Jackson ImmunoResearch Labs, West Grove, PA, USA). Images shown in the figures were representative of 5 individuals. NIH ImageJ software (Bethesda, MA, USA) was used for image acquisition and densitometric analysis of the gels.

### Quantitative PCR (RT-qPCR)

Total RNA was extracted using miRNeasy mini kit or RNeasy kit (Qiagen, Hilden, Germany). Complementary DNA (cDNA) was randomly primed from total RNA using the Omniscript reverse transcription kit (Qiagen). Quantitative PCR (RT-qPCR) were performed in duplicates with QuantiTect SYBR Green PCR Kit (Qiagen). All primers were purchased from Qiagen. Data

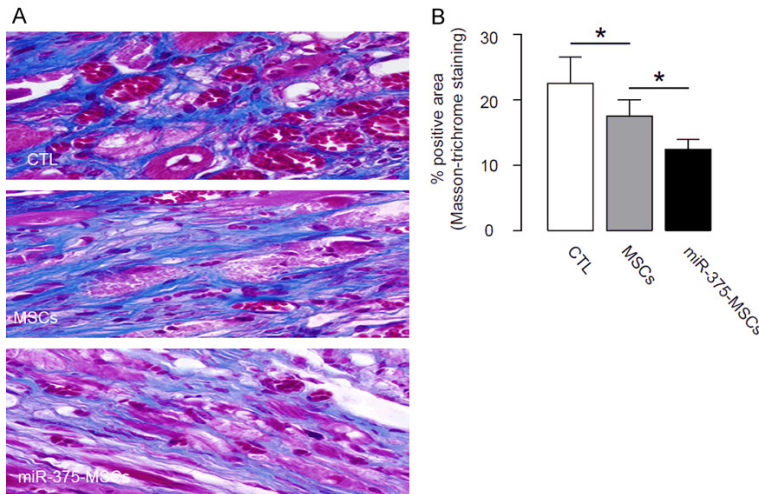


**Figure 3.** Transplantation of miR-375-MSCs further decreases the fibrosis after injury in mice. The effects of transplantation of miR-375-MSCs, or control MSCs on the fibrosis were examined two weeks after injury among control (CTL, injury only), MSC transplanted (MSCs), and miR-375-MSCs transplanted (miR-375-MSCs) mice. (A, B) Masson-trichrome staining for fibrosis was shown by representative images (A), and quantification (B). \* $p < 0.05$ .  $N=10$ .

were collected and analyzed using 2- $\Delta\Delta C_t$  method for quantification of the relative mRNA expression levels. Values of genes were first normalized against  $\beta$ -actin, and then compared to experimental controls.

#### MicroRNA target prediction and 3'-UTR luciferase-reporter assay

MiRNAs targets were predicted with the algorithms TargetSan (<https://www.targetscan.org>) [30]. Luciferase-reporters were successfully constructed using molecular cloning technology. The TIMP-1 3'-UTR reporter plasmid (TIMP-1 3'-UTR) and TIMP-1 3'-UTR reporter plasmid with a mutant at the miR-375 binding site (TIMP-1 3'-UTR mut) were purchased from Creative Biogene (Shirley, NY, USA). MSCs were co-transfected with TIMP-1 3'-UTR/TIMP-1 3'-UTR mut and miR-375/null by Lipofectamine 2000 ( $5 \times 10^4$  cells per well). Cells were collected 24 hours after transfection for assay using the dual-luciferase reporter assay system gene assay kit (Promega, Beijing, China), according to the manufacturer's instructions. The normalized control was null-transfected MSCs with 3'-UTR of TIMP-1 mRNA (wild type).

#### Statistical analysis

All statistical analyses were carried out using the SPSS 17.0 statistical software package. All

values are depicted as mean  $\pm$  SD and are considered significant if  $p < 0.05$ . All data were statistically analyzed using one-way ANOVA with a Bonferroni correction, followed by Fisher's Exact Test for comparison of two groups.

## Results

### Preparation of miR-375-expressing MSCs

Here, we aimed to increase the activity and functions of MSCs to improve their effects during scar formation. Since TIMP-1 has been reported as a negative regulator of MSC function, we screened TIMP-1-targeting miRNAs, and specifically found a candidate miR-

375, which binds to 3'-UTR of TIMP-1 mRNA at 124th-130th base site (Figure 1A), for modification of TIMP-1 levels in MSCs. MSCs were transduced with AAV carrying miR-375 (Figure 1B) and a GFP reporter and successfully purified for miR-375-expressing MSCs by flow cytometry based on GFP (Figure 1C). We found that miR-375-expressing MSCs expressed significantly higher levels of miR-375 (Figure 1D). In order to prove regulation of TIMP-1 levels by miR-375 in MSCs, MSCs cells were then transfected with 1  $\mu$ g plasmids of miR-375-expressing plasmids and plasmids carrying a luciferase reporter for 3'-UTR of TIMP-1 mRNA or a luciferase reporter for 3'-UTR of TIMP-1 mRNA with mutate at the miR-375 binding site (mut). The luciferase activities were determined in these cells, and our data showed that TIMP-1 3'-UTR plus miR-375 had the most repression for TIMP-1, and the 3'-UTR TIMP-1 mutant plus miR-375 had much lower repression (Figure 1E). These data demonstrate that miR-375 may target 3'-UTR of TIMP-1 mRNA to inhibit its translation in MSCs.

### miR-375-expressing MSCs have reduced TIMP-1

Then we analyzed TIMP-1 levels in miR-375-expressing MSCs, and found that although the mRNA levels of TIMP-1 in miR-375-MSCs cells

## MSCs-miR-375 to prevent scar formation

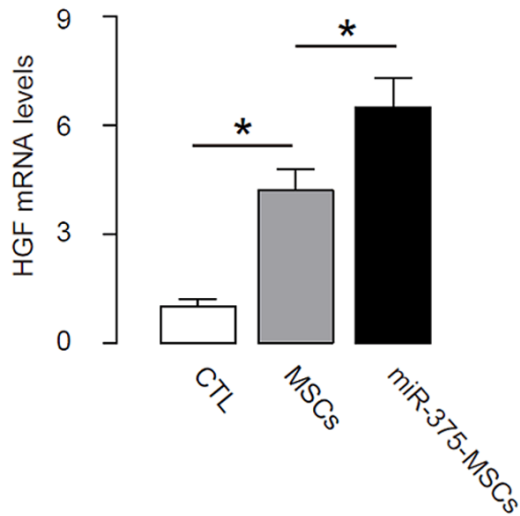


**Figure 4.** MiR-375-MSCs increase levels of HGF. The levels of HGF mRNA at the site of injury were examined among control (CTL, injury only), MSC transplanted (MSCs), and miR-375-MSCs transplanted (miR-375-MSCs). \* $p < 0.05$ . N=10.

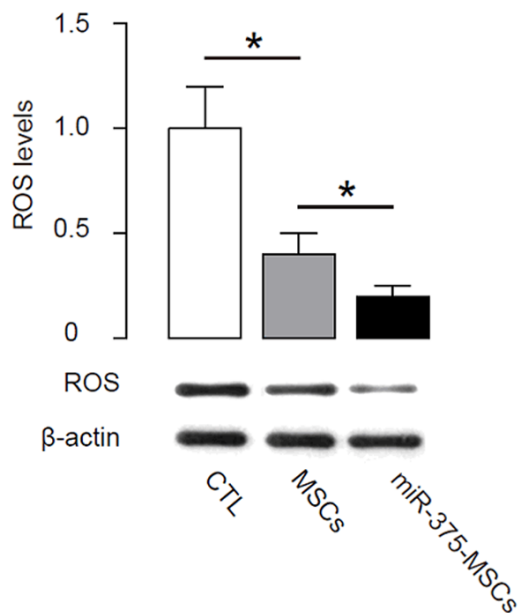


**Figure 5.** MiR-375-MSCs decrease levels of ROS. The levels of ROS were examined at the site of injury among control (CTL, injury only), MSC transplanted (MSCs), and miR-375-MSCs transplanted (miR-375-MSCs) mice, shown by representative images and quantification. \* $p < 0.05$ . N=10.

were unchanged (**Figure 2A**), the protein of TIMP-1 in miR-375-MSCs cells were significantly reduced (by more than 60%, **Figure 2B**). These data suggest that overexpression of

miR-375 in MSCs significantly decreases TIMP-1 protein expression. Then miR-375-MSCs were subjected to differentiation assays to confirm the MSC-phenotype after miR-375 overexpression. We performed Von kossa staining to evaluate osteogenic induction, Oil red O staining to evaluate adipogenic induction and Alcian blue staining to evaluate chondrogenetic induction (**Figure 2C-E**). Our data confirmed the maintenance of the MSC phenotype of miR-375-MSCs.

### *Transplantation of miR-375-MSCs further decreases the fibrosis after injury in mice*

Then we evaluated the effects of transplantation of miR-375-MSCs, or control MSCs on the fibrosis two weeks after injury in mice. We performed a Masson-trichrome staining, and we found that transplantation of MSCs significantly reduced the fibrosis at the site of injury. Moreover, the reduction in fibrosis was further reduced in mice grafted with miR-375-MSCs, shown by representative images (**Figure 3A**), and quantification (**Figure 3B**). Thus, these data suggest that transplantation of miR-375-MSCs further improves the anti-scar effects of MSCs.

### *MiR-375-MSCs increase levels of HGF*

Then we examined the mechanisms underlying the improved anti-scar effects of miR-375-MSCs. HGF has been shown as an anti-scar factor. We found that transplantation of MSCs significantly increased the levels of HGF mRNA at the site of injury. Moreover, the levels of HGF at the site of injury were even higher in mice grafted with miR-375-MSCs (**Figure 4**). Thus, these data suggest that transplantation of miR-375-MSCs may increase HGF levels to improve the anti-scar effects of MSCs.

### *MiR-375-MSCs decrease levels of ROS*

ROS has been associated with serious scar formation. Then, we examined the levels of ROS at the site of injury. We found that transplantation of MSCs significantly decreased the levels of ROS at the site of injury. Moreover, the levels of ROS at the site of injury were even lower in mice grafted with miR-375-MSCs, shown by representative images and quantification (**Figure 5**). Thus, these data suggest that transplantation of miR-375-MSCs may also decrease ROS levels to improve the anti-scar effects of MSCs.

## MSCs-miR-375 to prevent scar formation

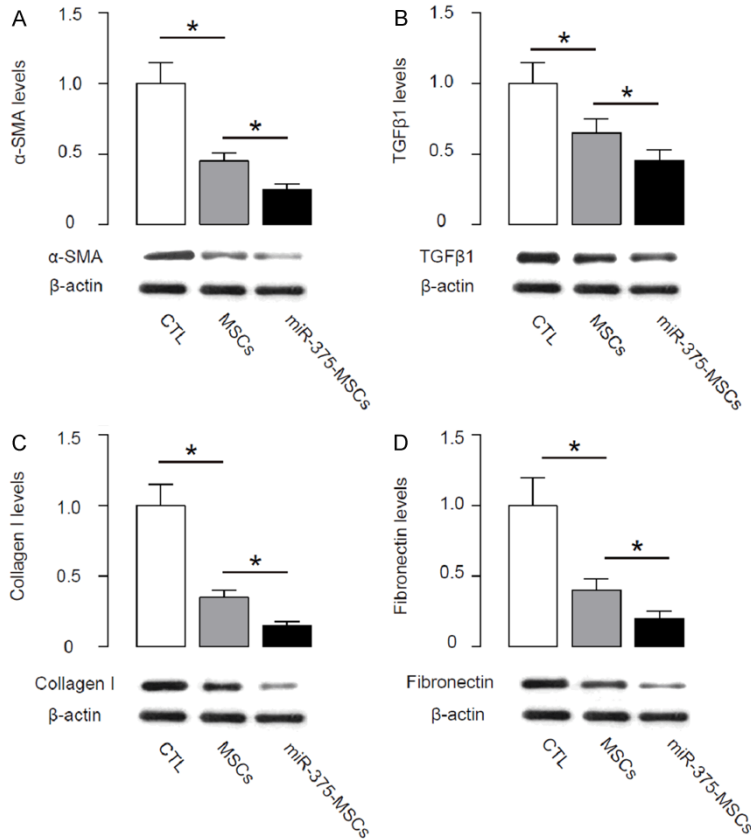


**Figure 6.** MiR-375-MSCs suppress myofibroblast transition. (A-D) The levels of α-SMA (A), TGFβ (B), Collagen I (C) and Fibronectin (D) were examined at the site of injury among control (CTL, injury only), MSC transplanted (MSCs), and miR-375-MSCs transplanted (miR-375-MSCs) mice, shown by representative images and quantification. \*p < 0.05. N=10.

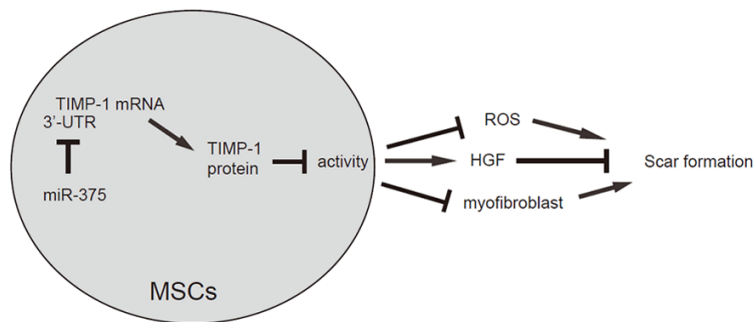


**Figure 7.** Schematic of the model. Transplantation of miR-375-expressing MSCs may significantly reduce the scar-associated fibrosis, possibly through reduction of ROS, suppression of transition of myofibroblasts from fibroblasts, and increases in HGF.

### miR-375-MSCs suppress myofibroblast transition

Transition of myofibroblasts from fibroblasts has been associated with serious scar forma-

tion. Then, we addressed to this question. Since α-SMA and TGFβ are a specific marker and a secreted protein by myofibroblasts, respectively, we analyzed the levels of these two proteins, as well as two fibrotic marker Collagen I and Fibronectin at the site of injury. We found that transplantation of MSCs significantly decreased the levels of α-SMA (Figure 6A), TGFβ (Figure 6B), Collagen I (Figure 6C) and Fibronectin (Figure 6D) at the site of injury. Moreover, the levels of α-SMA (Figure 6A), TGFβ (Figure 6B), Collagen I (Figure 6C) and Fibronectin (Figure 6D) at the site of injury were even lower in mice grafted with miR-375-MSCs. Thus, these data suggest that transplantation of miR-375-MSCs may also suppress myofibroblast transition from fibroblasts to improve the anti-scar effects of MSCs. Our findings were then summarized in a schematic, showing that transplantation of miR-375-expressing MSCs may significantly reduce the scar-associated fibrosis, possibly through reduction of ROS, suppression of transition of myofibroblasts from fibroblasts, and increases in HGF (Figure 7).

### Discussion

A previous study has shown that TIMP-1 regulates MSC functions and inhibition of TIMP-1 in MSCs significantly promotes MSC growth and differentiation into adult cells of the osteogenic lineage [17]. TIMP-1 is secreted from MSCs

at relatively high levels and knockdown of TIMP-1 production in MSCs up-regulates the stability, nuclear translocation, and promoter activity of β-catenin, suggesting that TIMP-1 is an inhibitor of β-catenin-dependent signaling [17]. The

Wnt/ $\beta$ -catenin signaling pathway is closely associated with the growth and development of MSCs, which is related to osteogenic differentiation of MSCs [17]. However, the effects of TIMP-1 attenuation on MSC effects on scar formation have not been extensively studied at molecular level, and an easy and robust way to knockdown TIMP-1 levels in MSCs is not available.

In the current study, we screened all TIMP-1-targeting miRNAs to select the one that could efficiently attenuate TIMP-1 levels in MSCs. Using bioinformatics analysis and a dual luciferase reporter assay, we showed that miR-375 could bind to TIMP-1 mRNA and significantly decrease its protein translation. However, the effects of miR-375 on MSCs may not only be conducted through TIMP-1, since its 3'-UTR of mRNA targets of miR-375 may include factors other than TIMP-1. In the future, further analyses of these factors may provide a more complete understanding of the role of miR-375 in MSCs.

Our next approach was to evaluate the effects of miR-375-mediated attenuation of TIMP-1 on the scar formation. We showed compelling data to demonstrate that miR-375-mediated attenuation of TIMP-1 significantly enhanced the effects of MSCs on reduction of fibrosis at the site of injury. Moreover, reduction of ROS, suppression of transition of myofibroblasts from fibroblasts and increases in HGF seem to all contribute to the effects of miR-375-mediated attenuation of TIMP-1 in MSCs.

To summarize, here we provided evidence to demonstrate a possibility of modification of MSC activity and function in attenuating scar formation after injury. Our study sheds new light on a scar-less wound healing.

### Acknowledgements

This work was supported by Important Medical Funded Projects of Hebei Province Health Department (NO. zd2013095) and Hebei Province Medical Follow-up Project 2014.

### Disclosure of conflict of interest

None.

**Address correspondence to:** Guoying Miao, Department of Dermatology, Affiliated Hospital of Hebei

University of Engineering, 81 Congtai Road, Handan 056029, China. Tel: +863108572000; Fax: +8631-08572000; E-mail: guoyingmiao@163.com; guoying\_miao@163.com

### References

- [1] Ud-Din S, Volk SW and Bayat A. Regenerative healing, scar-free healing and scar formation across the species: current concepts and future perspectives. *Exp Dermatol* 2014; 23: 615-619.
- [2] DiPietro LA. Angiogenesis and scar formation in healing wounds. *Curr Opin Rheumatol* 2013; 25: 87-91.
- [3] Leung A, Crombleholme TM and Keswani SG. Fetal wound healing: implications for minimal scar formation. *Curr Opin Pediatr* 2012; 24: 371-378.
- [4] Zipori D. Mesenchymal stem cells: harnessing cell plasticity to tissue and organ repair. *Blood Cells Mol Dis* 2004; 33: 211-215.
- [5] Li B, Shao Q, Ji D, Li F and Chen G. Mesenchymal Stem Cells Mitigate Cirrhosis through BMP7. *Cell Physiol Biochem* 2015; 35: 433-440.
- [6] Liu W, Zhang S, Gu S, Sang L and Dai C. Mesenchymal Stem Cells Recruit Macrophages to Alleviate Experimental Colitis Through TGFbeta1. *Cell Physiol Biochem* 2015; 35: 858-865.
- [7] Zhang J, Wu Y, Chen A and Zhao Q. Mesenchymal stem cells promote cardiac muscle repair via enhanced neovascularization. *Cell Physiol Biochem* 2015; 35: 1219-1229.
- [8] Song X, Xie S, Lu K and Wang C. Mesenchymal stem cells alleviate experimental asthma by inducing polarization of alveolar macrophages. *Inflammation* 2015; 38: 485-492.
- [9] Cao X, Han ZB, Zhao H and Liu Q. Transplantation of mesenchymal stem cells recruits trophic macrophages to induce pancreatic beta cell regeneration in diabetic mice. *Int J Biochem Cell Biol* 2014; 53: 372-379.
- [10] Lan A, Qi Y and Du J. Akt2 mediates TGF-beta1-induced epithelial to mesenchymal transition by deactivating GSK3beta/snail signaling pathway in renal tubular epithelial cells. *Cell Physiol Biochem* 2014; 34: 368-382.
- [11] Sun T, Gao GZ, Li RF, Li X, Li DW, Wu SS, Yeo AE and Jin B. Bone marrow-derived mesenchymal stem cell transplantation ameliorates oxidative stress and restores intestinal mucosal permeability in chemically induced colitis in mice. *Am J Transl Res* 2015; 7: 891-901.
- [12] Chen YL, Sun CK, Tsai TH, Chang LT, Leu S, Zhen YY, Sheu JJ, Chua S, Yeh KH, Lu HI, Chang HW, Lee FY and Yip HK. Adipose-derived mesenchymal stem cells embedded in platelet-rich

## MSCs-miR-375 to prevent scar formation

- fibrin scaffolds promote angiogenesis, preserve heart function, and reduce left ventricular remodeling in rat acute myocardial infarction. *Am J Transl Res* 2015; 7: 781-803.
- [13] Sun CK, Leu S, Hsu SY, Zhen YY, Chang LT, Tsai CY, Chen YL, Chen YT, Tsai TH, Lee FY, Sheu JJ, Chang HW and Yip HK. Mixed serum-deprived and normal adipose-derived mesenchymal stem cells against acute lung ischemia-reperfusion injury in rats. *Am J Transl Res* 2015; 7: 209-231.
- [14] Chen T, Zhang P, Fan W, Qian F, Pei L, Xu S, Zou Z, Ni B and Zhang Y. Co-transplantation with mesenchymal stem cells expressing a SDF-1/HOXB4 fusion protein markedly improves hematopoietic stem cell engraftment and hematogenesis in irradiated mice. *Am J Transl Res* 2014; 6: 691-702.
- [15] Chen HH, Chang CL, Lin KC, Sung PH, Chai HT, Zhen YY, Chen YC, Wu YC, Leu S, Tsai TH, Chen CH, Chang HW and Yip HK. Melatonin augments apoptotic adipose-derived mesenchymal stem cell treatment against sepsis-induced acute lung injury. *Am J Transl Res* 2014; 6: 439-458.
- [16] Jackson WM, Nesti LJ and Tuan RS. Mesenchymal stem cell therapy for attenuation of scar formation during wound healing. *Stem Cell Res Ther* 2012; 3: 20.
- [17] Egea V, Zahler S, Rieth N, Neth P, Popp T, Kehe K, Jochum M and Ries C. Tissue inhibitor of metalloproteinase-1 (TIMP-1) regulates mesenchymal stem cells through let-7f microRNA and Wnt/beta-catenin signaling. *Proc Natl Acad Sci U S A* 2012; 109: E309-316.
- [18] Ries C. Cytokine functions of TIMP-1. *Cell Mol Life Sci* 2014; 71: 659-672.
- [19] Bodden MK, Windsor LJ, Caterina NC, Yermovsky A, Birkedal-Hansen B, Galazka G, Engler JA and Birkedal-Hansen H. Analysis of the TIMP-1/FIB-CL complex. *Ann N Y Acad Sci* 1994; 732: 84-95.
- [20] Arthur MJ and Iredale JP. Hepatic lipocytes, TIMP-1 and liver fibrosis. *J R Coll Physicians Lond* 1994; 28: 200-208.
- [21] Di Leva G and Croce CM. miRNA profiling of cancer. *Curr Opin Genet Dev* 2013; 23: 3-11.
- [22] Pereira DM, Rodrigues PM, Borralho PM and Rodrigues CM. Delivering the promise of miRNA cancer therapeutics. *Drug Discov Today* 2013; 18: 282-289.
- [23] Mei Q, Li F, Quan H, Liu Y and Xu H. Busulfan inhibits growth of human osteosarcoma through miR-200 family microRNAs in vitro and in vivo. *Cancer Sci* 2014; 105: 755-762.
- [24] Wang F, Xiao W, Sun J, Han D and Zhu Y. MiRNA-181c inhibits EGFR-signaling-dependent MMP9 activation via suppressing Akt phosphorylation in glioblastoma. *Tumour Biol* 2014; 35: 8653-8658.
- [25] Liu G, Jiang C, Li D, Wang R and Wang W. MiRNA-34a inhibits EGFR-signaling-dependent MMP7 activation in gastric cancer. *Tumour Biol* 2014; 35: 9801-9806.
- [26] Dumortier O, Hinault C, Gautier N, Patouraux S, Casamento V and Van Obberghen E. Maternal protein restriction leads to pancreatic failure in offspring: role of misexpressed microRNA-375. *Diabetes* 2014; 63: 3416-3427.
- [27] Zhang N, Lin JK, Chen J, Liu XF, Liu JL, Luo HS, Li YQ and Cui S. MicroRNA 375 mediates the signaling pathway of corticotropin-releasing factor (CRF) regulating pro-opiomelanocortin (POMC) expression by targeting mitogen-activated protein kinase 8. *J Biol Chem* 2013; 288: 10361-10373.
- [28] Keller DM, Clark EA and Goodman RH. Regulation of microRNA-375 by cAMP in pancreatic beta-cells. *Mol Endocrinol* 2012; 26: 989-999.
- [29] Shi ZC, Chu XR, Wu YG, Wu JH, Lu CW, Lu RX, Ding MC and Mao NF. MicroRNA-375 functions as a tumor suppressor in osteosarcoma by targeting PIK3CA. *Tumour Biol* 2015; 36: 8579-8584.
- [30] Coronello C and Benos PV. ComiR: Combinatorial microRNA target prediction tool. *Nucleic Acids Res* 2013; 41: W159-164.